



# Spatial distribution of pollution characteristics and human health risk assessment of exposure to heavy elements in road dust from different functional areas of Zhengzhou, China

Huilang Wang<sup>1,2</sup> · Chenyang Shen<sup>1</sup> · Yongfei Kang<sup>1</sup> · Qiao Deng<sup>3</sup> · Xiaoying Lin<sup>1</sup>

Received: 16 December 2019 / Accepted: 17 April 2020 / Published online: 6 May 2020  
© Springer-Verlag GmbH Germany, part of Springer Nature 2020

## Abstract

Road dust from different sources directly contacts the human body and has potential effects on public health. In this study, a total number of 87 road dust samples were collected at 29 sampling sites from five different functional areas (commercial area (CA), residential area (RA), educational area (EA), industrial area (IA), and park area (PA)) in Zhengzhou to study the contamination status, distribution, source identification, ecological risk assessment, and spatial distribution of human health risks due to eight heavy elements. The geo-accumulation index ( $I_{geo}$ ) and pollution index (PI) revealed that there was very high contamination with Cd and Hg caused by atmospheric deposition, which should be paid special attention. Additionally, the source identification indicated that Cr, Ni, Cu, Zn, Cd, and Pb originate from anthropogenic activities related to traffic, and Hg can originate from medical equipment and agricultural chemicals, while the extremely low level of pollution with As could be explained by geographic sources. Moreover, the calculated ecological risk index values were increased in the order of CA > RA > EA > IA > PA in different functional areas. According to the human health risks of the whole city, children exposed to Pb have the highest health risk, especially for CA and IA, as calculated by the noncarcinogenic hazard index (HI). For adults and children, health risks caused by Cu, Zn, and Pb were higher in the CA, RA, and PA of the downtown area, whereas Cr and Ni had the highest noncarcinogenic exposure risk in northwestern Zhengzhou due to point source pollution. Calculations of the carcinogenic risk (CR) values for Cr, Ni, As, and Cd indicate that the value of Cr is highest ( $1.17 \times 10^{-7}$ ), especially inside the industrial area ( $8.55 \times 10^{-7}$ ), which is close to the lower limit of the threshold values ( $10^{-6}$  to  $10^{-4}$ ). These results can provide a theoretical basis and data support for air treatment, pollution control, and the implementation of public prevention in different functional areas of Zhengzhou.

**Keywords** Urban road dust · Heavy element contamination · Source identification · Ecological risk · Human risk spatial distribution

Responsible Editor: Philipp Gariguess

**Electronic supplementary material** The online version of this article (<https://doi.org/10.1007/s11356-020-08942-7>) contains supplementary material, which is available to authorized users.

✉ Xiaoying Lin  
linxiaoying@zzu.edu.cn

<sup>1</sup> College of Water Conservancy Engineering, Zhengzhou University, Zhengzhou, Henan 450001, People's Republic of China

<sup>2</sup> Zhengzhou Key Laboratory of Water Resource and Environment, Zhengzhou, Henan 450001, People's Republic of China

<sup>3</sup> Henan GRG Metrology & Test Co, LTD, Zhengzhou, Henan 450001, People's Republic of China

## Introduction

Atmospheric environmental pollution in urban areas has gained considerable attention from scholars and scientific researchers in recent decades, since it is closely relevant to people's daily lives and traffic and causes severe harm to the human body and low visibility (Liu et al. 2019). Studies of the content of fine particulate matter (PM<sub>2.5</sub>) (Cooper et al. 2019; Wang et al. 2020), organic contaminants, such as polycyclic aromatic hydrocarbons (PAHs) (Ma et al. 2019; Škrbić et al. 2019; Wang et al. 2016b), polybrominated diphenyl ethers (PBDEs) (Chou et al. 2019), and phthalate esters (PAEs) (He et al. 2019; Škrbić et al. 2016), and heavy metals (HM) (Cai et al. 2019; Lanzerstorfer and Logiewa 2019), such as zinc, lead, nickel, and cadmium, have been used for

measuring air pollution. Contaminants absorbed into fine particles could subside to the ground under the action of atmospheric pressure and gravity via road deposition via diffusion, transportation, and the aggregation process in the atmosphere (Wang et al. 2016b). Moreover, due to the advancement of urbanization, impermeable pavement has become an increasingly ubiquitous transportation facility in cities, which intensifies the accumulation of dust with pollutants. As an indicator of atmospheric dry deposition, urban road dust is an essential factor that undermines the ambient air quality and topsoil (Gąsiorek et al. 2017) and deep soil quality along roads (Ghanavati et al. 2019; Trujillo-González et al. 2016) as well as the quality of the receiving water body (Gunawardena et al. 2013; Zhao et al. 2010), which may cause adverse potential health risks to residents (Roy et al. 2019). Vehicles and crowds on impervious urban roads could generate considerable dust plumes (Škrbić et al. 2018), which will be resuspended into the atmosphere and cause airborne pollution and even haze due to wind (Shabanda et al. 2019). The resuspended particles and accumulated organic pollutants may be precipitated in the soil along roads (Taylor et al. 2010) and cause soil contamination, for which remediation is difficult (Ma et al. 2016b). Moreover, the contaminated road sediments in rainwater runoff during precipitation increases the burden on the assimilative capacity of rivers or receiving waters (Liu et al. 2018).

Due to their toxicity, persistence, and bioaccumulation, heavy elements in road dust in excessive concentrations have detrimental effects on the respiratory tract, gastrointestinal system, liver, endocrine function, cardiovascular center, and hematopoietic system (Rahman et al. 2019) and even low concentrations of road dust in some metals, such as lead, could cause neurological and developmental disorders (Mohmand et al. 2015). In recent decades, researchers have been investigating the characteristics of HMs in urban dust (Chen et al. 2014; Li et al. 2016a; Yang et al. 2019). Duong and Lee (2011) discovered considerable contaminating levels of cadmium, zinc, and nickel and a very high contamination of copper in road dust from asphalt highways in the metropolitan city of Ulsan, according to the contamination factor. By using positive matrix factorization (PMF) for a quantitative source analysis in Beijing, China, Men et al. (2018b) discovered that traffic-related exhaust gas accounted for 34.47% of the pollution sources; coal combustion and metal materials each accounted for approximately 25% of the pollution sources; and the use of pesticides, fertilizers, and medical equipment accounted for 14.88% of the pollution sources. Subsequently, more scholars considered the seasonal or spatial variation (Duan et al. 2018; Škrbić et al. 2018; Srikanth and Rao 2014; Zhang et al. 2015) and determined that the meteorological condition and intensity of human activities changed with the change in seasons, which causes a variations in the pollution conditions and main contamination source in different seasons (Men et al. 2018a). Moreover, road sediment particles

polluted by heavy elements, especially fine particles, can be absorbed by adults or children by ingestion, inhalation via the mouth and nose, dermal adsorption, and inhalation of mercury vapor, which potentially or directly affects human health (Lin et al. 2019; Torghabeh et al. 2019). The integrated hazard index values for children at four locations in the city of Kuala Lumpur were calculated as  $> 1$ , which indicates a possible noncarcinogenic effect (Wahab et al. 2020). Therefore, an investigation of the impact of various heavy elements concentrations in road dust on human health in Zhengzhou, a megalopolis of China, has great significance.

Due to the variety of human activities, land use types, and vehicle volumes among different functional areas in cities, the ambient environment and degree of contamination could display high spatial divergence (Trujillo-González et al. 2016; Wang et al. 2016c). Wang et al. (2016a) calculated the Tomlinson Pollution Load Index and geo-accumulation index of trace metals in urban dust of the Nanjing park area, which indicate that the dust samples in Nanjing park were extremely contaminated with lead. By studying the heavy metals in street dust from busy traffic areas with different characteristics, Duong and Lee (2011) discovered that traffic volume, atmospheric dispersion from traffic rotaries, industrial emissions, and the frequency of brake use and vehicles coming to a complete stop are factors that affect the contaminating levels of heavy metals in urban road dust. Arsenic was indicated as the most dangerous element based on a risk assessment for indoor and outdoor dust of the city (Huang et al. 2014). In spatial distribution analysis, previous studies have focused on heavy element concentrations, and corresponding ideal results have been obtained (Cai et al. 2019; Chen et al. 2014; Duan et al. 2018). However, the values of hazard quotient (HQ), hazard risk (HI), and cancer risk (CR) rather than the concentrations of heavy elements are significant in the assessment of carcinogenic and noncarcinogenic risk to human health (Ma et al. 2016a). Therefore, a study of the spatial distribution of health risk by different exposure pathways to humans in different functional areas has research meaning.

In this paper, to provide a scientific theoretical basis for the implementation of mitigation measures, treatment of heavy element pollution, and protection of urban residents, research has been carried out with the following aims: (1) road dust samples from different functional areas in Zhengzhou were collected, and descriptive statistical results were applied to analyze the distribution characteristics of the heavy element concentrations; (2) the pollution degree of different heavy elements in street dust of the study area were evaluated, and the ecological risk was assessed; (3) the contamination source of heavy elements in road dust was identified using the Pearson correlation coefficient and principal component analysis; (4) the spatial distribution of the health risk to children and adults from exposure to heavy elements in street dust was analyzed.

## Materials and methods

### Study area

Zhengzhou (112.7°–114.2° E, 34.3°–34.9° N), the provincial capital city of Henan, is not only a megalopolis in the central region of China but also an essential national comprehensive transportation hub and trade and logistics center, which might explain why the population in Zhengzhou is so large. Globalization and innovation increasingly provide conditions for urban development, and the geography, natural endowments, politics, institutions, history, and economic structure in Zhengzhou continue to play key roles in attracting more people to visit or settle in the city. By December 2018, Zhengzhou had a total resident population of 10.136 million, 11.41 million tourists, more than 4,000,000 registered motor vehicles, and more than 3,000,000 nonmotor vehicles; thus, urban road environment problems caused by excessive human activities and traffic congestion are inevitable. Zhengzhou has a north temperate continental monsoon climate with an average annual temperature of 15.6 °C and average annual precipitation of 542.15 mm. Zhengzhou is hottest in August, with a monthly mean temperature of 25.9 °C; the coldest month is January, with a monthly average temperature of 2.15 °C. The four seasons are distinctive, and summer and winter have a longer duration. Zhengzhou is located in the middle and lower reaches of the Yellow River and the northeast of the Funiu mountains to the Huanghuai plain transition zone with high ground in the west and middle and low grounds in the east.

### Sample collection

According to the overall layout of functional areas, Zhengzhou, as a city with rapid population and commercial development, has more commercial areas (CA), park areas (PA), and residential areas (RA) but fewer educational areas (EA) and industrial areas (IA). After analyzing the fundamental information of the study area, 29 sampling points were identified as shown in Fig. 1. Of the 29 sampling points, 7 points are in the CA and 7 points in PA, 6 points in RA, 5 points in EA, and 4 points in IA. The conditions of each sampling site, such as its location, function area, and detail of human activities and traffic flows, are listed in Table S1. To gain a comprehensive understanding of the pollution situation at every research site, a total of 87 road dust samples were collected at 29 sampling sites (3 subsamples for each site) from five different functional areas of Zhengzhou in June 2019. All the road dust samples were collected within a distance of approximately 10 m along the roadside; the weight of each sample was > 100 g (Men et al. 2018b). Since the length of the previous dry period has an impact on the particle size composition and concentration of sediment particles (Li et al. 2015; Zafra et al. 2017), all the analytical samples were

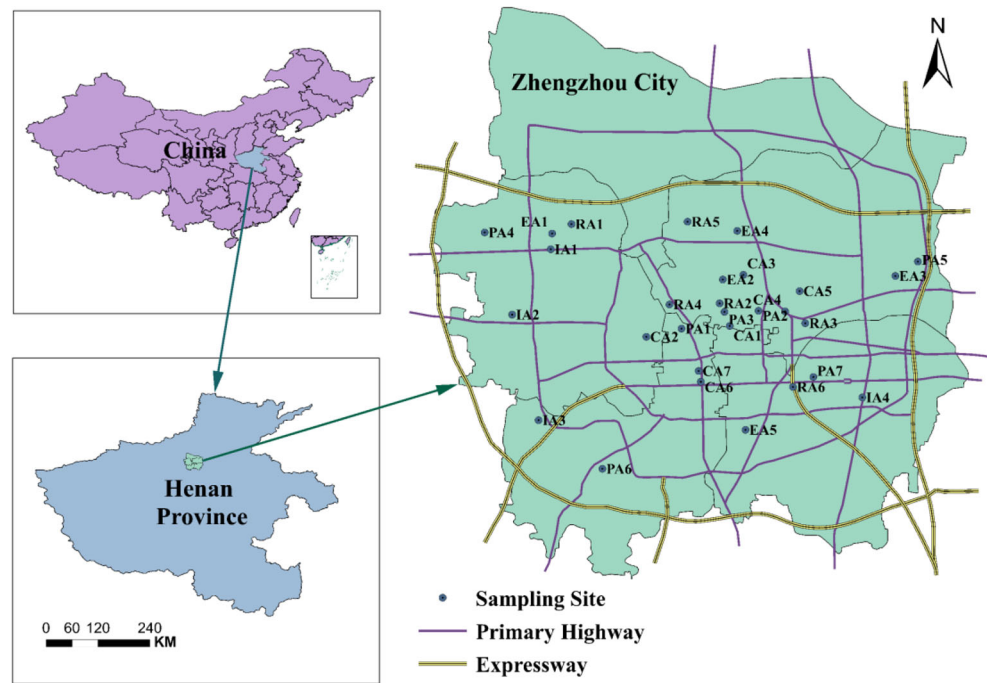
gathered after at least 3 dry days. Plastic brushes and dustpans were employed for collection, and the samples were placed in self-sealing polyethylene bags with a clean hairbrush, labeled, and then transferred to a laboratory as soon as possible. The sealed samples were stored in a refrigerator at 4 °C before they were analyzed.

### Experimental analysis

The samples were air dried for 5 days and passed through a 100-mesh polystyrene sieve (< 150 µm) to remove all debris, including stone, leaves, and hair (Lin et al. 2019). The < 150-µm-diameter fraction was selected for analysis because these particles are capable of remaining in the atmosphere for considerable durations, (Kurt-Karakus 2012; Li et al. 2015; Ma et al. 2016b) and the proportion of heavy elements in the atmosphere is larger; so the highest possible risk to human health is considered. In their study of the particle size distribution of street dust, Zhao et al. (2014) demonstrated that the median road dust sediment diameter,  $d_{50}$ , was less than 149 µm in the central urban area. Subsequently, parts of the sieved dust samples were transported to new self-sealing polyethylene bags and then stored at 4 °C before analysis. According to previous assessments of the potential health risk of heavy elements to the human body (Men et al. 2018b), seven typical metals (Li et al. 2017; Lin et al. 2019; Weerasundara et al. 2018) and arsenic, an oncogenic metalloid (Rahman et al. 2019; Škrbić et al. 2018), which has some of the chemical properties of a metal, were chosen for determination. These eight elements are cadmium (Cd), chromium (Cr), copper (Cu), mercury (Hg), nickel (Ni), lead (Pb), zinc (Zn), and arsenic (As).

To measure the concentration of Cd, Cr, Cu, Ni, Pb, and Zn, 0.1 g dust was taken extracted from each sample, placed in 50 ml polytetrafluoroethylene digestion vessels, and then dissolved with HNO<sub>3</sub> (5 ml)-HF (3 ml)-HClO<sub>4</sub> (2 ml) on a graphite digestion apparatus in the fume hood. The extracted samples were removed when sticky and digested with HCl (0.5 ml) when the extracted samples cooled. The digestion solutions were diluted with ultrapure water to a final volume of 25 ml in a colorimetric tube for analysis by inductively coupled plasma-mass spectrometry (ICP-MS Agilent 7700X) (HJ 766- 2015). For the detection of As and Hg, 0.5 g of dust of all the samples were placed in a colorimetric tube (50 ml). Afterwards, the mixture of ultrapure water and aqua regia (1:1 ratio in 10 ml) was added in sequence, digested in an electric-heated thermostatic water bath with lids at 100 °C for 2 h, and shaken once every half hour. After cooling, the samples were diluted to scale and placed on a spectrometer for As concentration measurement. The Hg content was determined by atomic fluorescence spectrometry (HJ 680-2013).

**Fig. 1** The distribution of 29 sampling sites from five different functional areas in Zhengzhou, China



**QA/QC (quality assurance/quality control)**

During the analysis process of the samples, 10% certified reference materials (CRMs) ( $N = 9$ ), 10% repeated samples ( $N = 9$ ), and 2% blank samples ( $N = 2$ ) were performed with the same treatment to ensure the accuracy and precision of the experiment (HJ 803- 2016). The series of CRMs for the chemical composition of soil (GSS 1-31), which were developed by Geophysical and Geochemical Prospecting Institute of Academy of Geological Sciences of Chinese, are mainly used as the reference standard of geology, geochemical and mineral survey, and for the quality monitoring in China. The Luochuan loess of Shanxi Province (GSS-8), soil of Liaohe Plain (GSS-11), and soil of Huabei Plain (GSS-13) were selected for QA/QC in this study. The concentration levels of elements in each reference material and the concentration levels determined in this study are shown in Table S2. Via data analysis, the concentration of the standard materials measured in the experiment is within the uncertainty range. The limit of detection (LOD) and limit of quantitation (LOQ) of the determination method and the repeatability of the parallel samples, which was indicated by relative standard deviation (RSD, in %), are shown in Table S3. During the data analysis, a standard curve was established with the correlation coefficient  $> 0.999$ , and an intermediate concentration point of standard curve was analyzed for every 20 samples (RSD values between the measured result and the actual concentration were  $< 10\%$ ) (HJ 803- 2016). Besides, the two blank samples were found to be undetectable heavy metal levels that were clearly below the method LOD values.

**Statistical analysis**

The descriptive statistical analysis of concentration of the measured samples was obtained by operating the IBM SPSS statistics 22 software package, which was also employed for identification of the pollution sources via factor analysis and calculation of the coefficients and significance level of the correlation matrix. In addition, the Origin 9.1 software was employed to analyze the holistic data of different factors and perform relevant graphics rendering. The spatial distribution of sampling sites and hazard index values for adults and children in study area were described by using ArcGIS 10.2. The ordinary kriging (OK) (Men et al. 2018b) and inverse distance weighted (IDW) (Škrbić et al. 2018) method can be applied for a spatial variation analysis. The geostatistical interpolation method of OK is selected to analyze the spatial distribution of the human health risk in this study because it can assign different weights to each sample grade based on the sample positions and degree of correlation among samples and then calculate the sliding weighted average of interpolation points.

**Pollution evaluation indices of urban dust quality**

The geo-accumulation index ( $I_{geo}$ ), namely, the Müller index (Müller 1981), considers not only the influence of the background value for the natural geological process but also the impact of human activities on heavy elements pollution. The Müller index has been employed to continuously determine the pollution levels in soil and road dust (Li et al. 2015; Škrbić et al. 2018). The equation is expressed as

$$I_{geo} = \log_2(C_n/1.5B_n) \tag{1}$$

where  $C_n$  is the concentration of the element  $n$  measured in dust samples, and  $B_n$  represents the background value of soil in Zhengzhou, China. The modified index 1.5, is usually applied to characterize the sedimentary characteristics, petrogeology, and other background values influences (Li et al. 2015; Men et al. 2018b; Weerasundara et al. 2018). The evaluation criterions of the geological accumulation index are listed in Table 1.

The pollution index (PI) is a contamination factor for assessing the degree of heavy elements pollution in road dust (Duong and Lee 2011). This index can be utilized for a given element in a certain sampling point (Men et al. 2018a).

$$PI = C_n/B_n \tag{2}$$

where  $C_n$  and  $B_n$  have the same values as previously noted and belong to the same unit. Five categories of PI exist to estimate the following heavy elements contamination levels: no contamination ( $PI < 1$ ), low level of contamination ( $1 \leq PI < 2$ ), middle level of contamination ( $2 \leq PI < 3$ ), considerable contamination ( $3 \leq PI < 6$ ), and very high level of contamination ( $6 \leq PI$ ).

### Ecological risk and human health risk assessment

#### Ecological risk

The ecological risk index (RI) evaluation method of heavy elements proposed by Hakanson (1980) has been applied to assess the contamination degree in soil and urban road dust (Men et al. 2018b). RI can be computed by using the following equation:

$$RI = \sum_{i=1}^n E_r^i \tag{3}$$

$$E_r^i = T_r^i \times C_f^i \tag{4}$$

$$C_f^i = C_n^i/B_n^i \tag{5}$$

where RI is the sum of eight ecological risk factors ( $E_r^i$ ) of heavy elements;  $E_r^i$  is the monomial potential ecological risk factor for element  $i$ ;  $T_r^i$  is the toxic response factor for a given material—1 for Zn; 2 for Cr; 5 for Cu, Ni, and Pb; 10 for As; 30 for Cd; and 40 for Hg (Hakanson 1980; Lin et al. 2019; Soltani et al. 2015; Zhao et al. 2014);  $C_f^i$  is the contamination factor of element  $i$  and numerically equal to the PI;  $C_n^i$  and  $B_n^i$  are the mean concentration of element  $i$  and its reference geographical background value, respectively, which are the same variables defined in Eqs. (1) and (2). The ecological risk levels are described as in Table 1 (Men et al. 2018b; Soltani et al. 2015).

#### Human health risk assessment

The assessment method can be applied to assess the noncarcinogenic or carcinogenic risk of human exposure to contaminated environmental media, such as heavy elements in dust in current conditions or future conditions (USEPA 1992; USEPA 2001). Children consume more food and water per unit of body weight, have a higher surface-to-volume ratio, grow at a faster rate, and have more rapidly changing hand-to-mouth behaviors and physiology changes than adults (USEPA 2009), which explains the significant difference of exposure risk between them (Shi et al. 2011). To determine the public health risks of urban road dust, people are grouped into adults and children according to the following four exposed pathways: mouth ingestion absorption, inhalation of resuspended particles via nose, dermal or eye contact with dust (USEPA 2003), and inhalation of Hg vapor (Lin et al. 2019). To assess the potential noncarcinogenic and carcinogenic risk of each element, the following equations were utilized to calculate:

**Noncarcinogenic risk** The assessment of the noncancer health risk values of each study element via the four exposure pathways was calculated using the following equations (Lin et al. 2019; USEPA 2001; Weerasundara et al. 2018):

$$AD_{ing} = C \times \frac{IngR \times EF \times ED}{BW \times AT} \times 10^{-6} \tag{6}$$

**Table 1** Contamination categories evaluation standard of the geo-accumulation index ( $I_{geo}$ ) (Müller 1981) and potential ecological risk level classification of  $E_r$  and RI values

$I_{geo}$ value	Pollution classes	Contamination status	$E_r$ or RI value	Risk levels
$I_{geo} < 0$	0	Practically uncontaminated	$E_r \leq 40$ ; $RI \leq 150$	Low potential ecological risk
$0 \leq I_{geo} < 1$	1	Uncontaminated to moderately contaminated	$40 < E_r \leq 80$ ; $150 < RI \leq 300$	Moderate potential ecological risk
$1 \leq I_{geo} < 2$	2	Moderately contaminated	$80 < E_r \leq 160$ ; $300 < RI \leq 600$	Considerable risk
$2 \leq I_{geo} < 3$	3	Moderately to heavily contaminated	$160 < E_r \leq 320$ ; $600 < RI$	High risk
$3 \leq I_{geo} < 4$	4	Heavily contaminated	$E_r > 320$	Extreme risk
$4 \leq I_{geo} < 5$	5	Heavily to extremely contaminated		
$5 \leq I_{geo}$	6	Extremely contaminated		

$$AD_{inh} = C \times \frac{InhR \times EF \times ED}{PEF \times BW \times AT} \tag{7}$$

$$AD_{dermal} = C \times \frac{SL \times SA \times ABS \times EF \times ED}{BW \times AT} \times 10^{-6} \tag{8}$$

$$AD_{vap} = C \times \frac{InhR \times EF \times ED}{VF \times BW \times AT} \tag{9}$$

where  $AD_{ing}$ ,  $AD_{inh}$ ,  $AD_{dermal}$ , and  $AD_{vap}$  are the average daily exposure amount of elements via ingestion, inhalation, dermal contact, and inhalation of vapors ( $mg/kg\ day^{-1}$ ), respectively;  $VF$  means a volatilization factor of  $32,675\ m^3/kg$  for Hg (Lin et al. 2019). Values of the other parameters for evaluating the risk of human exposure to urban road sediment in Eqs. (6)–(9) are shown in Table S4.

The hazard index (HI) is equal to the sum of the hazard quotients (HQs) that are calculated using the ratio of the average daily exposure dose via four exposure pathways to the reference dose for every element. The HI is employed to assess the accumulation of noncarcinogenic risk of a certain element (Li et al. 2017; Weerasundara et al. 2018).

$$HQ = \frac{AD_{ing/inh/dermal/vap}}{R_fD} \tag{10}$$

$$HI = \sum_{i=1}^4 HQ_i \tag{11}$$

where the specific reference dose ( $R_fD$ ,  $mg/kg\ day^{-1}$ ) threshold indicates the probability that a particular element contaminant will have a lifetime impact on human health (Mohmand et al. 2015; USEPA 2007).

$R_fD$  is based on the assumption that thresholds exist for certain toxic effects, such as cellular necrosis; the values of  $R_fD$  are listed in Table S5. If the value of  $HI < 1$ , the noncarcinogenic risk to human health is not significant. Values  $> 1$  suggest the strong possibility of occurrence of adverse noncarcinogenic effect risk to the public.

**Carcinogenic risk** The life average daily dose (LADD) for the cancer elements As, Cr, Ni, and Cd was computed for the inhalation exposure route using the following equation (USEPA 1992).

$$LADD = \frac{C \times EF}{AT \times PEF} \times \left( \frac{Inh_{child} \times ED_{child}}{BW_{child}} + \frac{Inh_{adult} \times ED_{adult}}{BW_{adult}} \right) \tag{12}$$

$$\text{Carcinogenic risk (CR)} = LADD \times SF \tag{13}$$

where  $C$  ( $mg/kg$ ) in Eqs. (6)–(9) and (12), combined with the values for the exposure factors, is considered to yield an estimation of the “reasonable maximum exposure” (USEPA 1989). Exposures were proposed to be estimated for a single exposure case (for both current and future land use) rather than

two exposure case of an average and an upper-bound exposure (USEPA 1989). The two cases approach measures the range of uncertainty surrounding these estimates to some extent, but the upper-bound estimate of exposure may be above the range of possible exposure and the average estimate is lower than exposures potentially experienced by much of the population (USEPA 1989). By analysis of the heavy element concentrations in 87 dust samples of Zhengzhou using SPSS22 software, the P-P plot of all element concentration values present the logarithmic normal distribution in this study. Therefore, the upper confidence limit (UCL) of the 95% confidence interval for the mean (Huang et al. 2014; Kurt-Karakus 2012; Li et al. 2017) were calculated to assess the highest exposure that is reasonably expected to occur at a site by the following equation. (Rahman et al. 2019; USEPA 1996)

$$C_{95\%UCL} = \exp\left(\bar{X} + 0.5s^2 + \frac{s \times H}{\sqrt{n-1}}\right) \tag{14}$$

where  $\bar{X}$  is the arithmetic mean of the log-transformed data,  $s$  is the standard deviation of the log-transformed data,  $H$  is the  $H$ -statistic (Gilbert 1987), and  $n$  is the number of samples.  $Inh_{child}$ ,  $ED_{child}$ , and  $BW_{child}$  are the parameter values for children, and  $Inh_{adult}$ ,  $ED_{adult}$ , and  $BW_{adult}$  are the corresponding parameter values for adults (Table S4).  $SF$  is the slope factor ( $mg/kg\ day^{-1}$ ) of a particular carcinogen; its values are displayed in Table S5.

$CR < 10^{-6}$  demonstrates that it could not pose a carcinogenic risk when exposure to heavy elements in road dust, while the potential carcinogenic risk is highly likely if  $CR > 10^{-4}$ . Some management measures to mitigate cancer risks should be implemented when  $CR$  ranges from  $10^{-6}$  to  $10^{-4}$  (Wahab et al. 2020).

## Results and discussion

### Total concentrations of heavy elements

The relative standard deviations (RSDs) of the three collected subsamples from a sampling site of Zhengzhou were generally within 10%, and some were slightly greater, which illustrates that the pollution conditions in different subsites of a sampling point are distinct. Therefore, considering the average detection value of the samples collected from three different subsites of a sampling site as the value of this sampling point is necessary. The descriptive statistics of eight heavy elements (HEs) concentration investigated in 29 sampling points with 87 street dust samples of Zhengzhou are provided in Table 2. The arithmetic mean value, which represents the average content of heavy elements in different samples, takes into account the concentration values of all locations. So, the arithmetic mean value is selected as an indicator for the comparison among

HEs (Fig. 2). The mean concentrations of the eight selected heavy elements in urban road dust samples collected from Zhengzhou generally decreased on the order of Zn > Pb > Cr > Cu > Ni > As > Hg > Cd, which is particularly similar to the regularity of other literatures (Mohmand et al. 2015). An analysis of HEs indicates road sediments generally have higher contents of Cr, Zn, and Pb, whose concentration values have a higher dispersion degree among the sampling points.

Although the zinc concentration was the highest in this study area, it was the lowest one compared with that in other Chinese and some foreign cities, except Ahvaz, Iran (Table 3). The Pb concentration in Zhengzhou is less than that in all the cities compared, except Dhaka, Bangladesh, which can be attributed to the decreased usage of leaded gasoline in recent years in Zhengzhou (Li et al. 2017). The concentrations of Cr, Ni, and Cu in this study area were less than those in other compared cities. On the other hand, the mean concentration of As in Zhengzhou urban road dust is higher than that of Beijing, China; Ahvaz, Iran; Dhaka, Bangladesh; and Novi Sad, Serbia, and more than the background values of Zhengzhou but lower than those of Guangzhou, Baoji, and Isfahan. The Cd pollution condition in street dust of Zhengzhou is similar to that in Beijing and Guiyang and similar to that in Novi Sad, Serbia and Beijing Park, China, while lower than that in other cities. In addition, the Hg content of street dust in the study area is slightly greater than that in Beijing and Guangzhou, which is nearly 5 times less than that in Baoji, China, and 10 times higher than the background value in Zhengzhou. No significant difference in the Hg concentration among different cities and different functional areas in Zhengzhou was likely caused by the volatility of Hg, which indicates that the cleaning mechanism of road sweeping cleaning or rainstorm rushing may not have an obvious influence on reducing the mercury content.

### Variety of different functional areas

Different functional areas with various land uses, human activities, traffic density, population density, energy

consumptions, and frequencies of road sweeping present the distinct pollution situations (Shabanda et al. 2019). The mean concentrations of HEs in road dust collected from five different functional areas (CA, IA, PA, EA, and RA) in Zhengzhou are presented in Table 3. A comparison of the total mean element concentrations in each functional area yields the following ranking in descending order: CA > RA > IA > EA > PA. This ranking is consistent with the conclusion of previous studies performed in Chengdu (Li et al. 2017), which may demonstrate that different cities are similar with regard to the relative influence of different functional areas. The heavy element content of CA is greater than that of other functional areas in cities, which can be attributed to the high public and traffic flow. In addition, the high density of high-rise buildings causes a rotation of contaminated particles in the air and accumulation of HEs in this area, which also contributes to the higher HE pollution in CA. The highest zinc concentration of dust samples in different functional area roads was detected in RA ( $163.85 \pm 133.36$  mg/kg) and much higher than that in EA ( $153.20 \pm 76.26$  mg/kg) and CA ( $145.25 \pm 57.84$  mg/kg). However, these concentrations were less than the concentration in the EA (278 mg/kg), which has the lowest Zn content in the Chengdu area (Li et al. 2017). An inspection of the table reveals that the Cr and Ni contents were highest in IA but lowest in PA, which suggests that both metals may be derived from the same source of pollution. Similarly, the concentrations of Cu, Hg, and Pb were highest in the CA while lowest in the PA. The concentrations of other heavy elements in the PA were the lowest, except As and Cd, which is probably due to the slight difference in the characteristics of arsenic and cadmium pollution in different functional areas.

### Pollution indices

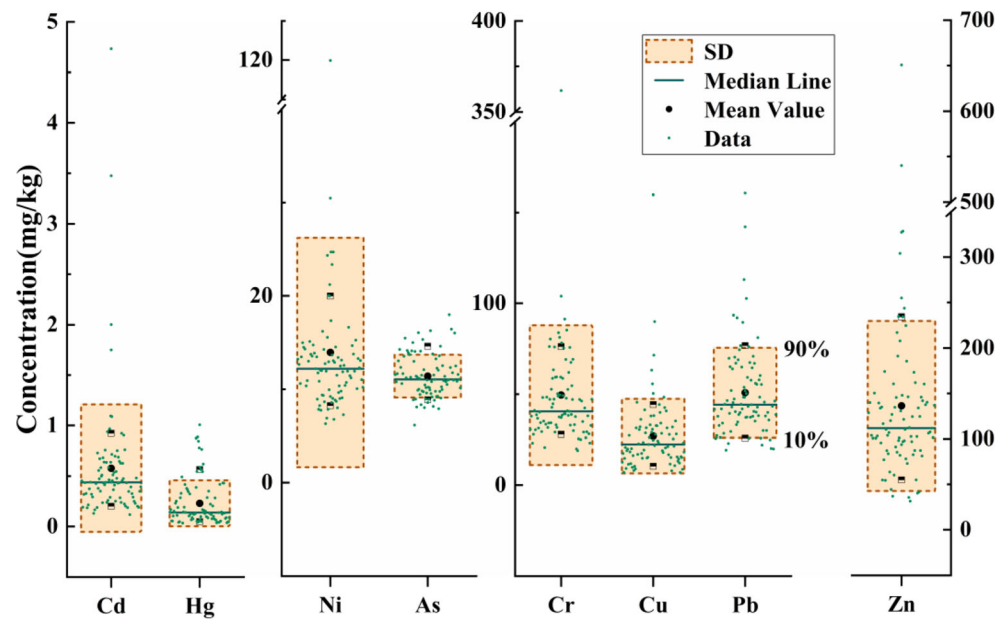
A boxplot of  $I_{geo}$  values of heavy elements in all the street dust samples ( $N = 87$ ) is shown in Fig. 3. The inter-quartile range (IQR) in Figs. 3 and 4 is the difference between the upper quartile (Q3, i.e., at 75%) and the lower quartile (Q1, i.e., at 25%) of the pollution indices values. Theoretically, the

**Table 2** Results of statistical analyses of eight heavy elements concentration (mg/kg) in road dust samples of Zhengzhou

Elements	Min	Max	Mean	Median	SD	CV	GM	95%UCL	Skewness	Kurtosis
Cr	19.00	361.81	49.56	40.58	38.45	0.78	43.78	57.76	6.42	51.26
Ni	6.31	119.89	13.95	12.20	12.28	0.88	12.42	16.57	7.67	65.93
Cu	6.98	159.76	26.98	22.45	20.48	0.76	22.50	31.34	3.74	20.68
Zn	31.49	650.64	136.30	111.69	93.61	0.69	116.58	156.26	3.14	13.39
As	6.16	17.98	11.41	11.05	2.30	0.20	11.19	11.90	0.57	0.06
Cd	0.12	4.73	0.58	0.44	0.63	1.09	0.45	0.71	4.72	26.36
Pb	19.31	160.62	50.87	44.21	24.77	0.49	46.24	56.15	1.93	5.37
Hg	0.03	1.01	0.23	0.14	0.23	1.00	0.15	0.28	1.68	2.23

SD standard deviation, CV coefficient of variance, GM geometric mean, 95%UCL the upper limit of the 95% confidence interval for the mean

**Fig. 2** Heavy elements concentration values of 87 road dust samples in Zhengzhou



outliers of a boxplot are detected by judging whether the data are in the range of the upper limit ( $Q3 + 1.5IQR$ ) and lower limit ( $Q1 - 1.5IQR$ ). Due to the existence of point source pollution in cities (Huang et al. 2015), the contamination degree of HE in different sampling sites varies, which may explain

why outliers exist in the pollution index values of some heavy elements. The analysis of outliers is conducive to the analysis and research on the point pollution situation of sampling sites in Zhengzhou. PI reflected the contamination levels of HEs in road deposition dust relative to urban soil and as shown in

**Table 3** Mean concentration of heavy elements in urban road dust from Zhengzhou, its different functional areas, and other reference cities (mg/kg)

Research area	Cr	Ni	Cu	Zn	As	Cd	Pb	Hg	Reference
Chengdu, China	84.3	24.4	100	296	NA	1.66	82.3	NA	Li et al. 2017
Beijing, China	92.10	32.47	83.12	280.65	4.88	0.59	60.88	0.16	Men et al. 2018b
Beijing Park, China	69.33	25.97	72.13	219.20	NA	0.64	201.82	NA	Du et al. 2013
Guangzhou, China	<i>176.22</i>	41.38	192.36	<i>1777.18</i>	20.05	2.14	387.53	0.22	Huang et al. 2014
Baoji, China	126.7	48.8	123.2	715.3	19.8	NA	<i>433.2</i>	<i>1.1</i>	Lu et al. 2010
Guiyang, China	129.04	60.43	129.33	176.05	NA	0.61	63.12	NA	Duan et al. 2018
Kandy, Sri Lanka	103.0	87.6	123.6	1116.9	NA	68.8	234.4	NA	Weerasundara et al. 2018
Isfahan, Iran	82.13	66.63	182.26	707.19	<i>22.15</i>	2.14	393.33	NA	Soltani et al. 2015
Ahvaz, Iran	115.84	NA	<i>207.6</i>	104.24	9.33	6.80	202.14	NA	Ghanavati et al. 2019
Dhaka, Bangladesh	144.34	37.01	49.68	239.16	8.09	11.64	18.99	NA	Rahman et al. 2019
Novi Sad, Serbia	60.1	28.1	42.7	NA	1.88	0.54	62.5	NA	Škrbić et al. 2018
Delhi, India	57.7	24.7	99.9	200.7	NA	NA	164.2	NA	Roy et al. 2019
Background soil values of Zhengzhou	64	21	14	42	8	0.08	18	0.023	
Background soil values of China	62.5	28.9	21.4	69.4	11.1	0.11	21.4	0.03	CNEMC 1990
Zhengzhou, China									
Mean values	49.56	13.95	26.98	136.30	11.41	0.58	50.87	0.23	This study
EA	37.73	13.41	22.88	153.20	<i>12.11</i>	<i>0.82</i>	47.28	0.20	
IA	<i>68.50</i>	<i>20.38</i>	18.49	131.91	10.98	0.43	57.05	0.19	
RA	47.69	13.30	31.82	<i>163.85</i>	11.50	0.48	50.42	0.29	
CA	63.56	13.44	<i>41.58</i>	145.25	10.41	0.70	<i>66.76</i>	<i>0.30</i>	
PA	34.80	11.72	16.01	94.20	12.07	0.45	34.38	0.15	

The italic font indicates the highest concentration in the areas compared (different cities around the world or different functional areas in Zhengzhou) NA not available



Fig. 4, its values of all the study elements follow the order of  $Hg > Cd > Zn > Pb > Cu > As > Cr > Ni$ .

Except for one subsample of IA1, which was collected inside the industrial area, all  $I_{geo}$  values of Ni and Cr in the study area were almost 0, which indicates that nickel and chromium pollution were not present in the road sediment in Zhengzhou City. The point of difference between the PI values and  $I_{geo}$  values for Cr and Ni evaluation is that low contamination ( $1 < PI < 2$ ) is presented in a limited number of sites, 16.1% and 6.9%, respectively. Additionally, the calculation results show that arsenic pollution in Zhengzhou is low ( $1 < PI < 2$ ) with a mean PI value of 1.43. Although the mean PI value of Cu is also  $< 2$ , the analysis indicates middle, considerable (CA4 and RA6), or even very high levels of pollution (CA1 and RA6) in some places, especially in commercial and residential areas.

In the Pb ranking, the contamination situation is moderate based on the average PI values (2.83) but rendered moderate to heavy levels of contamination ( $I_{geo} > 2$ ) or even a very high level of contamination ( $PI > 6$ ) in some commercial and industrial areas. The number of residents and vehicles, as well as industrial activities, may be the most dominant factor that causes this point source pollution phenomenon. Analogously, Zn, the metal with the highest average concentration, generally has a moderate level of pollution and has a high level of contamination status in locations with heavy traffic activities. The very high level of contamination of Zn in residential areas (RA2, RA3, and RA4) can be explained by the potential influence of heavy traffic in the central area and high frequency of human activity caused by the surrounding

numerous commercial areas (Gunawardena et al. 2013; Men et al. 2018b). In addition, the pollution levels of Cd and Hg in Zhengzhou were moderate to heavy on average, according to the  $I_{geo}$  values, and nearly one in three of the study areas was heavily contaminated ( $I_{geo} > 3$ ) with mercury, which warrants public awareness. A very high level of pollution was detected for Cd and Hg with mean PI values of 7.25 and 10, respectively. Further research is needed to explain the outliers in the CA, EA, and RA for cadmium and mercury pollution (Fig. 4). The point source pollution of Pb and Zn in some areas of Zhengzhou may be attributed to the significant pollution degree of historical accumulation in soil and the potential contamination of urban road dust by resuspension (Li et al. 2017). The atmosphere deposition of Cd and Hg in road dust of the Zhengzhou area warrants special attention.

### Identification of pollution sources

Because the HE concentrations of road dust obey a log-normal distribution, the Pearson's correlation coefficients for eight elements were calculated (Table 4) using the log-transformed data to study the correlation relationship among the metals in urban street dust samples. The homology and coherence information of metals can be evaluated (Lu et al. 2010; Soltani et al. 2015).

A high positive correlation at the 0.01 level is displayed in the group of Cr–Cu (0.787), which indicates that the origin and pathway of emission for this group are likely similar. Another group, Cr–Ni–Cu–Zn–Cd–Pb, shows significant correlations with each other at  $p < 0.01$ , especially Cr–Cu

**Fig. 3** Boxplot of Geo-accumulation values of each element in all road samples (N = 87) from Zhengzhou

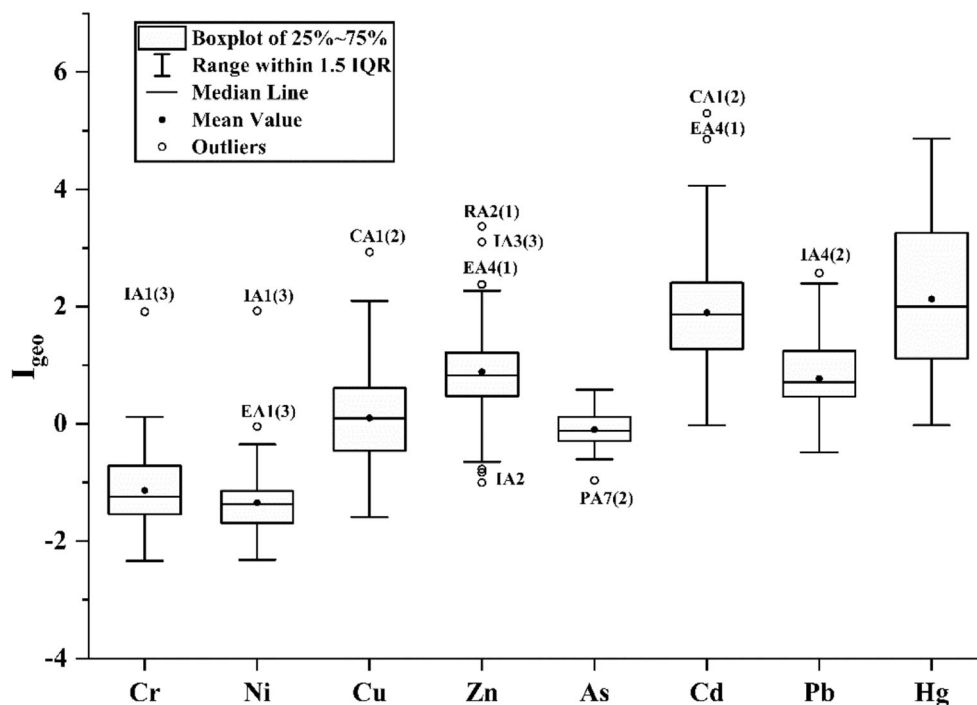
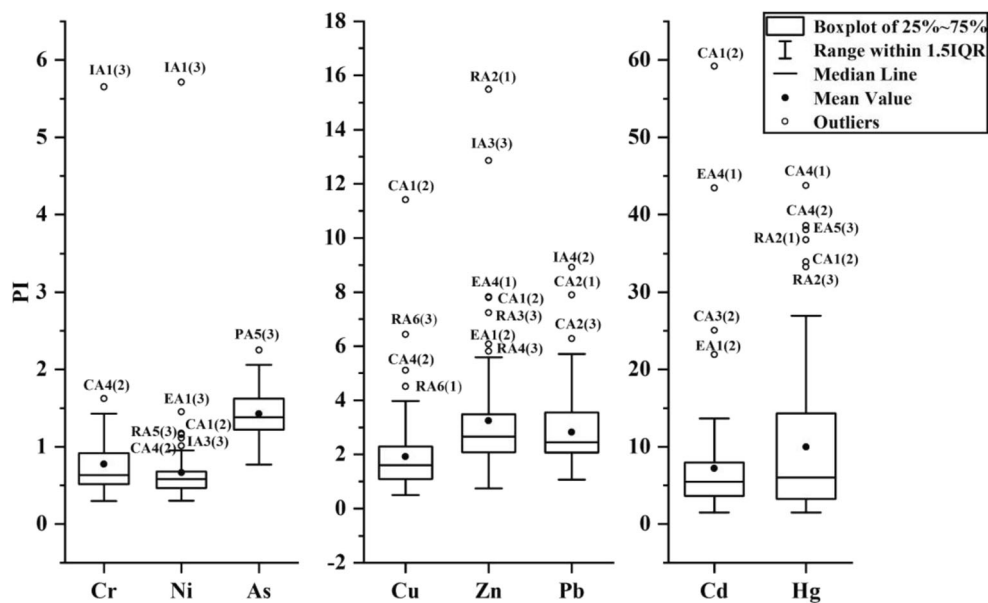


**Fig. 4** Boxplot of PI values of each element in all samples collected from different functional areas in Zhengzhou



(0.787), Cr–Zn (0.635), Cr–Pb (0.741), Ni–Zn (0.672), Ni–Cd (0.655), Cu–Zn (0.668), Cu–Pb (0.675), Zn–Cd (0.677), and Zn–Pb (0.640). However, arsenic does not present a significant correlation with any metal, according to the correlation coefficient analysis at the 0.01 level, except a low correlation with Cd (0.301). Moreover, another group of Hg with Cr (0.386), Cu (0.344), Zn (0.315), and Pb (0.331) has a low correlation at the 0.01 level, and the relationship of Hg and Ni is not significant (0.242) at the 0.05 level.

The principal component analysis (PCA) method was applied with the SPSS software for identification of the eight HE pollution sources (Guan et al. 2019). The Kaiser–Meyer–Olkin (KMO) and Bartlett tests on the logarithmic conversion data of HE concentration showed that the KMO measurement value was 0.806, and the significance level of the Bartlett test was 0.00, which suggests that the data were suitable for further

principal component analysis and factor analysis. The analysis results are shown in Table S6.

In the PCA, three principal components were extracted by the principal component method, and the component matrix was rotated by the maximum variance method proposed by Kaiser to minimize the number of variables with the highest load on each factor. The obtained three components accounted for 80.3%, among which the first component accounted for 45.4% (Fig. 5) of the total variance and the factor loadings were higher on Cr (0.728), Ni (0.825), Cu (0.706), Zn (0.864), Cd (0.832), and Pb (0.678) (Table S6). These results are consistent with the evaluation results based on the Pearson correlation coefficient, which shows that the five HMs are highly correlated and greatly contribute to factor 1. Based on previous studies, Cr, Ni, Cu, and Cd in road sediment were mainly caused by the weathering and corrosion of automobile parts

**Table 4** Pearson’s correlation coefficient matrix and corresponding significant level of all the analyzed heavy elements in road dust of Zhengzhou City

	Cr	Ni	Cu	Zn	As	Cd	Pb	Hg
Cr		0.000	0.000	0.000	0.995	0.000	0.000	0.000
Ni	0.584**		0.000	0.000	0.116	0.000	0.000	0.029
Cu	0.787**	0.500**		0.000	0.216	0.000	0.000	0.002
Zn	0.635**	0.672**	0.668**		0.177	0.000	0.000	0.004
As	–0.01	0.176	–0.139	0.152		0.006	0.695	0.081
Cd	0.438**	0.655**	0.403**	0.677**	0.301**		0.000	0.187
Pb	0.741**	0.417**	0.675**	0.640**	–0.044	0.440**		0.003
Hg	0.386**	0.242*	0.344**	0.315**	0.195	0.148	0.331**	

The left lower part is correlation coefficient; the right upper part is significant level

\*Significant correlation at the 0.05 level (2-tailed)

\*\*Significant correlation at the 0.01 level (2-tailed) (in italic)

and other metal materials, such as paint, guardrail, and coatings (Huang et al. 2014; Li et al. 2017; Škrbić et al. 2018). By analyzing the pollution sources of different heavy metals, Rahman et al. (2019) discovered that Zn was usually detected in tire tread rubber, car lubricants (Jin et al. 2019), and carburetors. Corrosion on the car surface and the widespread use of leaded gasoline and road paint can increase the lead levels in sediments (Roy et al. 2019). Moreover, the sources of these HMs are traffic-related emitters (Men et al. 2018b). Research by Gunawardena et al. (2013) revealed that zinc is related to traffic volume, whereas Pb, Cd, Ni, and Cu are related to traffic congestion. Consequently, factor 1 is more likely to be related to vehicle exhaust and transportation facilities from anthropogenic activities.

Component 2 is primarily loaded by Hg, which accounts for 18.8% of the total variance. The use of mercury-containing fertilizers and pesticides is one reason for the general increase in the mercury content in soil, water, and dust (Men et al. 2018b). Hg presented in fertilizers and pesticides could volatilize into the air, transport over a certain distance, and eventually sink to the ground (Dong et al. 2017; Men et al. 2019; Naderizadeh et al. 2016), which accelerates the Hg contamination in road dust. In addition, some medical equipment in hospitals and clinics, such as thermometers, sphygmomanometers, and amalgams utilized in dentistry and cinnabar, contain mercury (hydrargyrum), which will cause certain mercury pollution (Giersz et al. 2017; Li et al. 2016b). According to PI values, the Hg concentration in road dust is 10 times larger than soil background value in Zhengzhou, which indicates that human activities have a greater impact on the Hg content in urban dust. Based on the analysis of Hg use in cities, factor 2 can be attributed to anthropogenic origins, such as medical

facilities and agricultural fertilizers and pesticides rather than nature factors.

The proportion of component 3 overwhelmingly characterized by As is 16.1% of the total variance, which is consistent with the result of no significant correlation between arsenic and other elements and implies that As has a separate source of contamination. Strong anthropogenic activities, such as the application of biosolids and manures, ashes from coal combustion (Wuana and Okieimen 2011), and exploitation of oil field, have been demonstrated to be vital arsenic sources (Bai et al. 2019). Combined with the previous pollution index assessment of arsenic, arsenic pollution is extremely low in each sampling area of Zhengzhou. Hence, the main cause of the As pollution source (factor 3) might be preliminarily determined as the background value of natural conditions.

## Assessment of ecological and human health risk

### Ecological risk assessment

The  $E_r$  value represents the monomial potential ecological risk to the public of an element in street dust, while the RI value reveals the gross ecological risk of all HEs. The conclusion of analysis (Fig. 6) indicates that the ecological risks caused by Cr, Ni, Cu, Zn, As, and Pb are low ( $E_r < 40$ ). Conversely, the risk of cadmium is high based on the high value of  $I_{geo}$  217.5, and the risk of mercury is extreme ( $E_r > 320$ ), as indicated by the high pollution index (PI) of 400. For different functional areas, the potential ecological risk of Hg is extreme in the CA and RA, while the risk of Cd is higher in the CA and EA.

Overall, the degree of deviation of the RI values in different sampling sites substantially varies, which suggests the significant difference risks generated among the sample sites (Fig. 7). The analysis results indicate that the RI values and the sum of  $E_r$  in different functional areas were on the order of CA > RA > EA > IA > PA, which is similar to the order of the total element concentrations: CA > RA > IA > EA > PA. The higher is the heavy elements content, the greater is the potential for ecological risk. However, a larger difference of RI values in the CA could attribute to the diversity of prosperity and traffic in different business districts of Zhengzhou. Moreover, the risk levels evaluated with RI were classified as having considerable potential ecological risk in the PA and IA and high risk (RI > 600) in the CA, EA, and RA. This finding may be due to a relatively higher level of Cd emitted via commercial, educational, and residential building construction and the use of batteries, plastics, and automobile tires (Men et al. 2018b) and a higher level of Hg from the use of some devices of hospitals and clinics and amalgams in dentistry and cinnabar in the CA and RA.

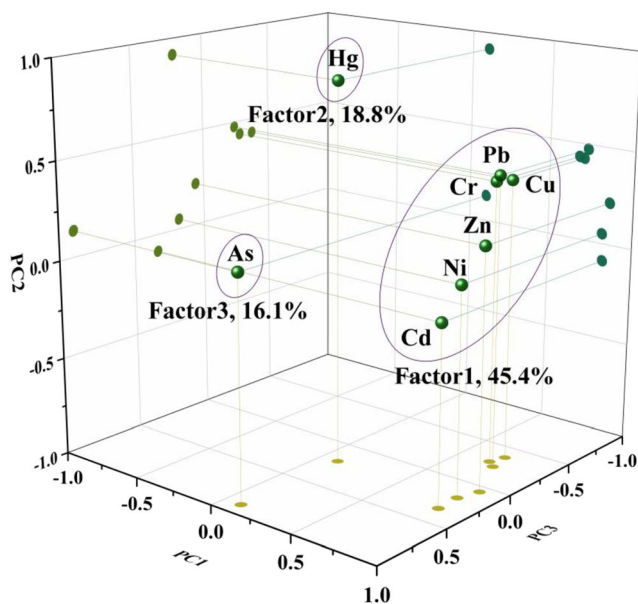
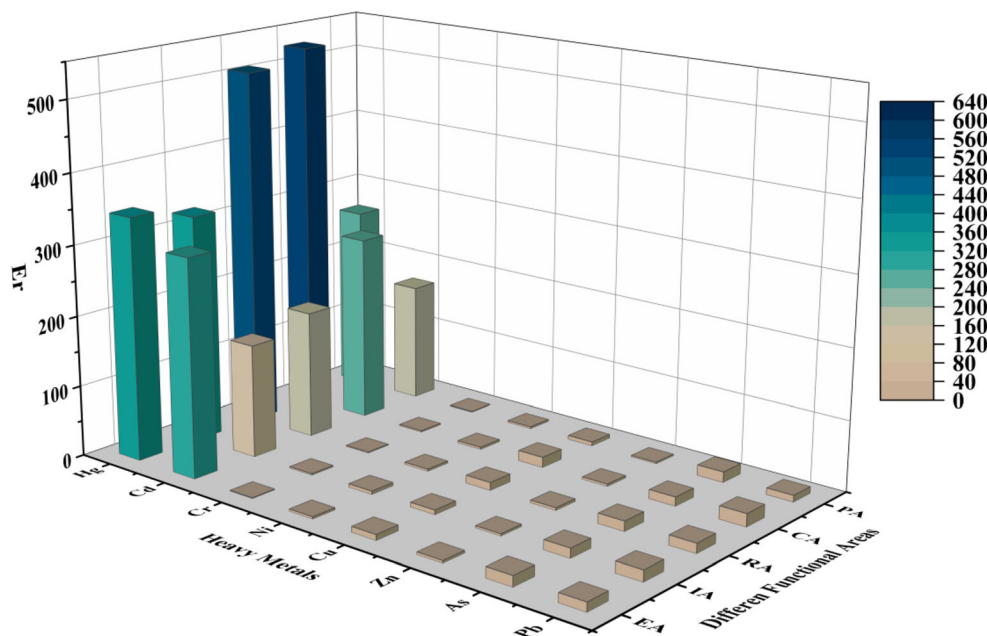


**Fig. 5** Three-dimensional scatter diagram of coefficient matrix of three extracted components (PC1, PC2, and PC3)

**Fig. 6** Monomial potential ecological risk ( $E_r$ ) values of each element in different functional areas



**Human health risk assessment**

To understand the degree of harm to the human body caused by heavy elements in road dust in Zhengzhou City via different exposure pathways, the health risk assessment model proposed by the US Environmental Protection Agency (USEPA) was employed to evaluate carcinogenic and noncarcinogenic risks to public health (USEPA 1989; USEPA 2017). The HQ and HI values of each heavy element in all samples were calculated using the model to comprehend the noncarcinogenic risk of exposure to adults and children at each study site. Several HQ values of descriptive statistical significance for each element for children and adult exposure are displayed in Table S7.

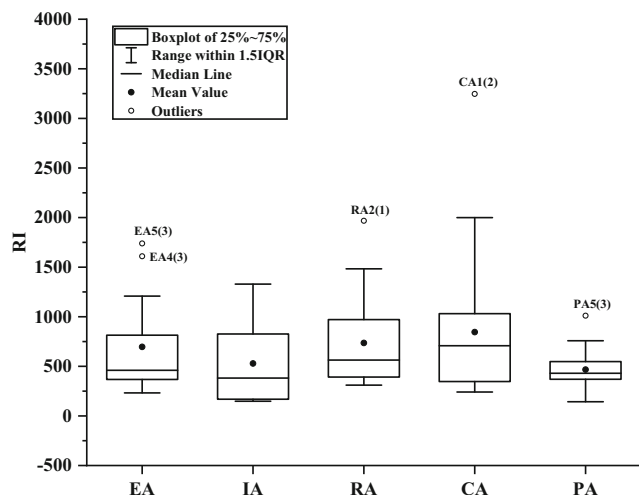


**Fig. 7** Boxplot of ecological risk index (RI) values in different functional areas

The USEPA (1996) declares that the noncarcinogenic risk can be disregarded if the HQ values were less than  $1 \times 10^{-6}$ , whereas remedial measures should be implemented if the values are sufficiently large and exceed  $1 \times 10^{-4}$  (Kurt-Karakus 2012). The HQ values of eight heavy elements for different exposure pathways were investigated. The results (Table S7) express that, for children and adults, the  $HQ_{ing}$  of all elements,  $HQ_{dermal}$  values of Cr, and  $HQ_{vapor}$  of Hg on average were larger than  $1 \times 10^{-4}$ . Of even greater concern is that the  $HQ_{ing}$  values of As for children and  $HQ_{ing}$  values of Pb for children and adults exceeded  $1 \times 10^{-2}$ . For the noncancer exposure risk to humans of Hg, according to the HQ values in different exposure pathways, the order of four exposure pathways were decreasing as follows: inhalation of vapor > ingestion > dermal contact > inhalation through mouth and nose. The results reveal that the reduction of the potential contamination of the vapor form of HM in the atmosphere is more difficult via road sweeping, which is a cleaning mechanism. On the other hand, for most other elements, the route of ingestion appears to be the primary exposure pathway of noncarcinogenic exposure risk for both children and adults in Zhengzhou, followed by dermal contact though exposure skin and inhalation via the mouth and nose. This finding is similar to that obtained by analyses of previous studies (Mohmand et al. 2015; Weerasundara et al. 2018) and underscores the reason people should pay attention to personal hygiene, reduce the frequency of hand-to-mouth behavior, and apply proper skin protection measures outdoors, especially for children with rapid bone growth and a higher exposure risk (Chen et al. 2014).

The HI values, which is the sum of the HQs in different exposure pathways, were calculated with the average values

of each heavy element in the road deposition samples for different functional areas. According to the analysis of the statistical data in Table 5, for adults and children, the order of the HI values of all heavy elements at risk in different functional areas is expressed as follows: CA > IA > RA > EA > PA. Although the noncancer risk index of each heavy element for children were an order of magnitude higher than that for adults in corresponding functional areas, no significant difference among the areas was observed. Among the heavy element exposure of the human body to urban dust in various functional areas, children have the highest noncarcinogenic exposure risk ( $HI > 0.1$ ) to lead in IA and CA. Moreover, Pb is deleterious to human health (Ackah 2019), even at low concentrations, by causing disruption to the nervous system and development. On the other hand, high blood Pb levels can replace  $Ca^{+}$  ions in bones, which causes bone deformity (Mohmand et al. 2015), especially for children, and could have destructive effects on the human nervous system, kidney, and brain tissues (Duan et al. 2018; Rahman et al. 2019). Therefore, people who are chronically exposed to industrial and commercial areas need extra protection, especially children.

The analysis reveals that the HI spatial distribution trend of each heavy element for both adults and children is consistent. Since children are more susceptible than adults, the hazard index for the same heavy element at the same concentration is greater for children than for adults (Ackah 2019). The spatial distributions of the HI values for children for each element are presented in Fig. 8 using the data of 29 sample sites (average of three subsampling points).

The HI values of Hg described in the distribution diagram indicate that children and adults are subjected to a higher

health risk in the middle of the study area and tiny discrepancy appeared between them with a 0.99 times lower risk to children than adults in the corresponding sites. Minor differences also arose in the HI values of Cr, Ni, As, and Cd with a 1.86, 2.24, 2.27, and 1.78 times, respectively, higher risk to children than adults. The spatial distribution of the noncancer hazard risk caused by Cd was higher in the northern of Zhengzhou and that of As was higher in the northern and western. The HI values of Ni and Cr were greater northwest of Zhengzhou, which may be due to the excessive metal content in the IA1(3) sample in the industrial area, where robots are mainly manufactured by using nickel hydride batteries or nickel–cadmium batteries and chromium alloys. Among children and adults, the largest disparities were observed in the risk values for Cu, Zn, and Pb at levels that were 9.30, 9.28, and 9.26 times, respectively, higher for children than adults, which is almost an order of magnitude higher. Whether in CA, RA, or PA, copper, zinc, and lead, which are typically related to the composition and use of automobiles (Yang et al. 2019), all pose larger health risks for both adults and children in the city central area of Zhengzhou. This phenomenon implies that a large noncancer health risk can be attributed to intense human activities, such as traffic congestion and large crowds. This finding also shows that HEs in road dust can influence the heavy elements content in the surrounding road sediment via certain diffusion (Men et al. 2018b).

The computation of the CR values of carcinogenic heavy elements, Cr, Ni, As, and Cd in this study, in all samples indicates that the cancer risk for Ni, As, and Cd could be negligible with an average CR value of  $6.59 \times 10^{-10}$ ,  $9.69 \times 10^{-10}$ , and  $2.05 \times 10^{-10}$ , respectively (Table 5), which were

**Table 5** HI values of each heavy element exposed to adults and children and CR values of carcinogenic element in different functional areas of Zhengzhou, China.

		EA		IA		RA		CA		PA	
		Adult	Children	Adult	Children	Adult	Children	Adult	Children	Adult	Children
HI	Cr	9.14E-03	1.70E-02	1.66E-02	3.09E-02	1.16E-02	2.15E-02	1.54E-01	2.87E-02	8.43E-03	1.57E-02
	Ni	1.86E-04	4.17E-04	2.83E-04	6.34E-04	1.84E-04	4.14E-04	1.86E-04	4.18E-04	1.62E-04	3.65E-04
	Cu	4.08E-04	3.80E-03	3.30E-04	3.07E-03	5.68E-04	5.28E-03	7.42E-04	6.90E-03	2.86E-04	2.66E-03
	Zn	3.67E-04	3.40E-03	3.16E-04	2.93E-03	3.93E-04	3.64E-03	3.48E-04	3.23E-03	2.26E-04	2.09E-03
	As	1.07E-02	2.43E-02	9.70E-03	2.20E-02	1.02E-02	2.31E-02	9.20E-03	2.09E-02	1.07E-02	2.42E-02
	Cd	9.91E-04	1.76E-03	5.14E-04	9.13E-04	5.79E-04	1.03E-03	8.45E-04	1.50E-03	5.40E-04	9.59E-04
	Pb	9.77E-03	9.05E-02	1.18E-02	1.09E-01	1.04E-02	9.65E-02	1.38E-02	1.28E-01	7.10E-03	6.58E-02
Sum of elements	Hg	1.04E-02	1.03E-02	9.79E-03	9.67E-03	1.54E-02	1.52E-02	1.60E-02	1.58E-03	7.98E-03	7.88E-03
		4.20E-02	1.52E-01	4.93E-02	1.79E-01	4.93E-02	1.67E-01	5.65E-02	2.05E-01	3.54E-02	1.20E-01
CR	Cr	8.91E-08		1.62E-07		1.13E-07		1.50E-07		8.22E-08	
	Ni	6.33E-10		9.63E-10		6.28E-10		6.35E-10		5.54E-10	
	As	1.03E-09		9.32E-10		9.76E-10		8.84E-10		1.03E-09	
	Cd	2.91E-10		1.51E-10		1.70E-10		2.48E-10		1.59E-10	

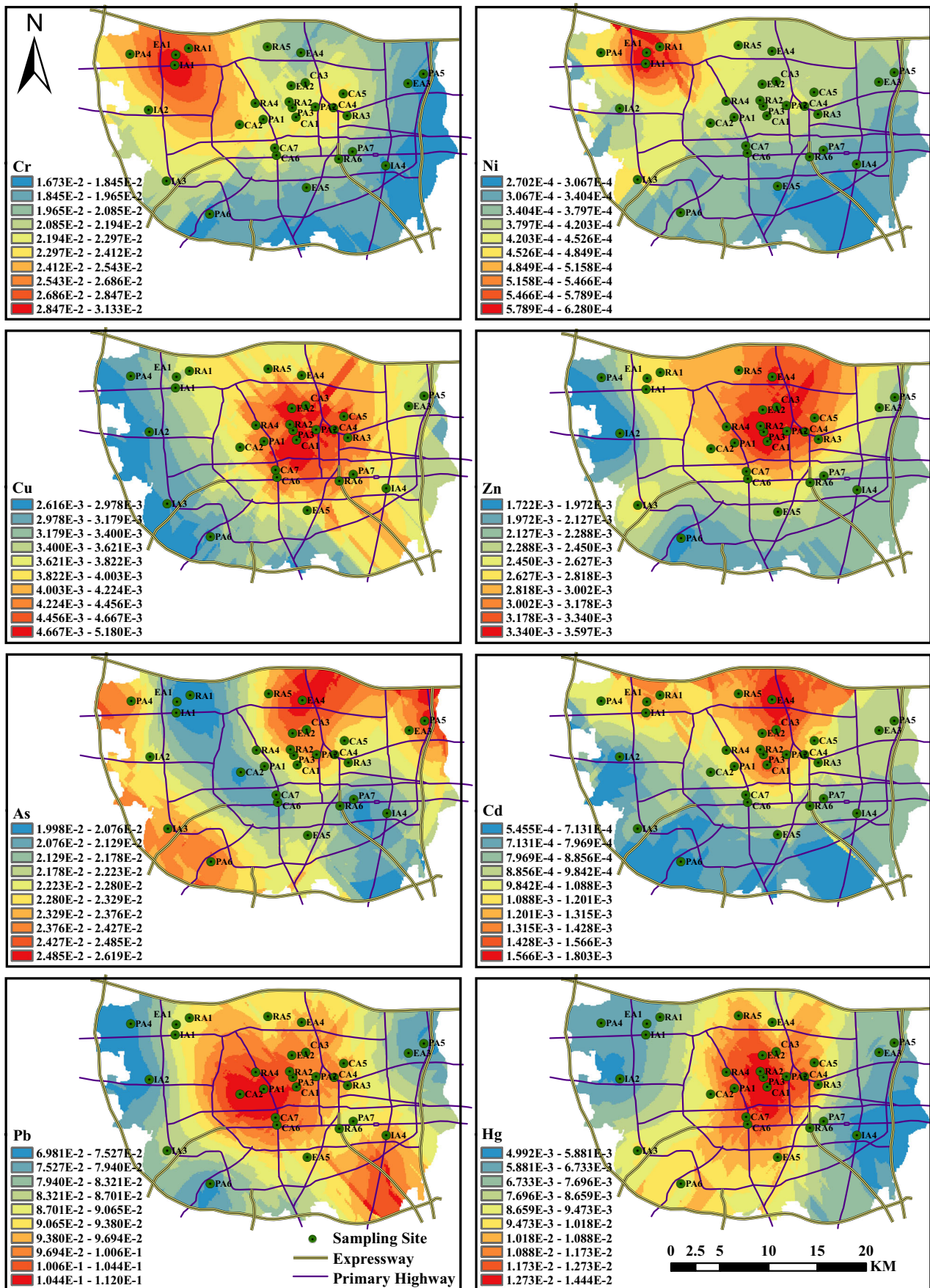


Fig. 8 Spatial distribution of HI values for each element exposed to children

under the lower limit of threshold values ( $10^{-6}$  to  $10^{-4}$ ). The higher value among them was the As exposure, and the most common adverse health effects of arsenic toxicity are skin lesions (melanosis, keratosis, and leucomelanosis), which are considered the early symptoms of arsenic poisoning (Shil and Singh 2019). The Cr ( $1.17 \times 10^{-7}$ ) cancer risk to the public in Zhengzhou was potentially close to the lower limit value ( $10^{-6}$ ), especially in the sample collected inside the industrial area with  $8.55 \times 10^{-7}$ . According to the CR values of the carcinogenic elements in the five different functional areas, the cancer health risks of Cr and Ni were the highest in the industrial area, followed by CA, RA or EA, and PA, which has a similar order of hazard index values. In addition, chromium is extensively employed to protect alloy surfaces and building materials, as well as electroplating, batteries, plastics, and fertilizers (Li et al. 2017). Thus, the commercial and educational building construction and the use of batteries and plastics in residential areas may explain the higher CR values of Cr in the EA, CA, and RA. Therefore, the cancer exposure risk to humans of Cr, especially in industrial areas, should be given substantial attention. Moreover, the health risk to the public posed by other pollutants, such as polycyclic aromatic hydrocarbons, PM<sub>2.5</sub>, or other undetected heavy metals, such as Mn and Fe, or in some high-pollution areas, such as mining area, should also be taken into account in a comprehensive assessment of the pollution risks for a city.

## Conclusions

The mean concentrations of Cr and Ni in 87 samples collected from five different functional areas were lower than the background values in Zhengzhou, while the Cd and Hg concentration values in road dust samples were 7.25 and 10 times greater, respectively, than the background values in soil. In addition, considerable pollution due to Pb was detected in the IA and CA, and the ecological risk in different functional areas was decreased in the following order: CA > RA > EA > IA > PA. Among the heavy element exposure of the human body to urban dust in various functional areas, the highest noncarcinogenic exposure risk (HI > 0.1) of children to lead in IA and CA was observed. Copper, zinc, and lead, which are typically related to the assembly and use of automobiles, pose larger health risks for both adults and children in the CA, RA, and PA of the downtown area in Zhengzhou. The highest noncarcinogenic exposure risk of Cr and Ni in northwestern Zhengzhou is due to point source pollution. It is noteworthy that the cancer risk value of Cr was more likely to be near the lower limit of the threshold value, especially inside the industrial area.

**Funding information** The research was financial supported by the National Natural Science Foundation of China (grant numbers 51879242 and 51739009).

## Compliance with ethical standards

**Conflict of interest** The authors declare that they have no conflict of interest.

## References

- Ackah M (2019) Soil elemental concentrations, geoaccumulation index, non-carcinogenic and carcinogenic risks in functional areas of an informal e-waste recycling area in Accra, Ghana. *Chemosphere* 235:908–917. <https://doi.org/10.1016/j.chemosphere.2019.07.014>
- Bai J, Zhao Q, Wang W, Wang X, Jia J, Cui B et al (2019) Arsenic and heavy metals pollution along a salinity gradient in drained coastal wetland soils: depth distributions, sources and toxic risks. *Ecol Indic* 96:91–98. <https://doi.org/10.1016/j.ecolind.2018.08.026>
- Cai K, Li C, Na S (2019) Spatial distribution, pollution source, and health risk assessment of heavy metals in atmospheric depositions: a case study from the sustainable city of Shijiazhuang, China. *Atmosphere* 10. <https://doi.org/10.3390/atmos10040222>
- Chen H, Lu X, Li LY (2014) Spatial distribution and risk assessment of metals in dust based on samples from nursery and primary schools of Xi'an, China. *Atmos Environ* 88:172–182. <https://doi.org/10.1016/j.atmosenv.2014.01.054>
- Chou TH, Ou MH, Wu TY, Chen DY, Shih YH (2019) Temporal and spatial surveys of polybromodiphenyl ethers (PBDEs) contamination of soil near a factory using PBDEs in northern Taiwan. *Chemosphere* 236:124117. <https://doi.org/10.1016/j.chemosphere.2019.06.087>
- CNEMC (1990) China National Environmental Monitoring Center. The backgrounds of soil environment in China. Environment Science Press of China
- Cooper N, Green D, Knibbs LD (2019) Inequalities in exposure to the air pollutants PM<sub>2.5</sub> and NO<sub>2</sub> in Australia. *Environ Res Lett* 14(11): 115005
- Dong H, Lin Z, Wan X, Feng L (2017) Risk assessment for the mercury polluted site near a pesticide plant in Changsha, Hunan, China. *Chemosphere* 169:333–341. <https://doi.org/10.1016/j.chemosphere.2016.11.084>
- Du Y, Gao B, Zhou H, Ju X, Hao H, Yin S (2013) Health risk assessment of heavy metals in road dusts in urban parks of Beijing, China. *Prog Environ Sci* 18:299–309. <https://doi.org/10.1016/j.proenv.2013.04.039>
- Duan Z, Wang J, Xuan B, Cai X, Zhang Y (2018) Spatial distribution and health risk assessment of heavy metals in urban road dust of Guiyang, China. *Nat Environ Pollut Technol* 17(2): 407–412
- Duong TT, Lee BK (2011) Determining contamination level of heavy metals in road dust from busy traffic areas with different characteristics. *J Environ Manag* 92:554–562. <https://doi.org/10.1016/j.jenvman.2010.09.010>
- Gąsiorek M, Kowalska J, Mazurek R, Pająk M (2017) Comprehensive assessment of heavy metal pollution in topsoil of historical urban park on an example of the Planty Park in Krakow (Poland). *Chemosphere* 179:148–158. <https://doi.org/10.1016/j.chemosphere.2017.03.106>
- Ghanavati N, Nazarpour A, De Vivo B (2019) Ecological and human health risk assessment of toxic metals in street dusts and surface

- soils in Ahvaz, Iran. *Environ Geochem Health* 41:875–891. <https://doi.org/10.1007/s10653-018-0184-y>
- Giersz J, Bartosiak M, Jankowski K (2017) Sensitive determination of Hg together with Mn, Fe, Cu by combined photochemical vapor generation and pneumatic nebulization in the programmable temperature spray chamber and inductively coupled plasma optical emission spectrometry. *Talanta* 167:279–285. <https://doi.org/10.1016/j.talanta.2017.02.018>
- Gilbert RO (1987) *Statistical methods for environmental pollution monitoring*. Van Nostrand Reinhold, New York, pp 177–185
- Guan Q, Zhao R, Pan N, Wang F, Yang Y, Luo H (2019) Source apportionment of heavy metals in farmland soil of Wuwei, China: comparison of three receptor models. *J Clean Prod* 237:117792. <https://doi.org/10.1016/j.jclepro.2019.117792>
- Gunawardena J, Egodawatta P, Ayoko GA, Goonetilleke A (2013) Atmospheric deposition as a source of heavy metals in urban stormwater. *Atmos Environ* 68:235–242. <https://doi.org/10.1016/j.atmosenv.2012.11.062>
- Hakanson L (1980) An ecological risk index for aquatic pollution control. A sedimentological approach. *Water Res* 14:975–1001. [https://doi.org/10.1016/0043-1354\(80\)90143-8](https://doi.org/10.1016/0043-1354(80)90143-8)
- He Y, Wang Q, He W, Xu F (2019) Phthalate esters (PAEs) in atmospheric particles around a large shallow natural lake (Lake Chaohu, China). *Sci Total Environ* 687:297–308. <https://doi.org/10.1016/j.scitotenv.2019.06.034>
- HJ 680-2013, Soil and sediment—determination of mercury, arsenic, selenium, bismuth, antimony—microwave dissolution/atomic fluorescence spectrometry. Ministry of Environmental Protection of the People's Republic of China (in Chinese)
- HJ 766-2015, Solid Waste—determination of metals—inductively coupled plasma mass spectrometry (ICP-MS). Ministry of Environmental Protection of the People's Republic of China (in Chinese)
- HJ 803-2016, Soil and sediment—determination of aqua regia extracts of 12 metal elements—inductively coupled plasma mass spectrometry. Ministry of Environmental Protection of the People's Republic of China (in Chinese)
- Huang M, Wang W, Chan CY, Cheung KC, Man YB, Wang X, Wong MH (2014) Contamination and risk assessment (based on bioaccessibility via ingestion and inhalation) of metal(loid)s in outdoor and indoor particles from urban centers of Guangzhou, China. *Sci Total Environ* 479-480:117–124. <https://doi.org/10.1016/j.scitotenv.2014.01.115>
- Huang Y, Li T, Wu C, He Z, Japenga J, Deng M, Yang X (2015) An integrated approach to assess heavy metal source apportionment in peri-urban agricultural soils. *J Hazard Mater* 299:540–549. <https://doi.org/10.1016/j.jhazmat.2015.07.041>
- Jin Y, O'Connor D, Ok YS, Tsang DC, Liu A, Hou D (2019) Assessment of sources of heavy metals in soil and dust at children's playgrounds in Beijing using GIS and multivariate statistical analysis. *Environ Int* 124:320–328. <https://doi.org/10.1016/j.envint.2019.01.024>
- Kurt-Karakus PB (2012) Determination of heavy metals in indoor dust from Istanbul, Turkey: estimation of the health risk. *Environ Int* 50:47–55. <https://doi.org/10.1016/j.envint.2012.09.011>
- Lanzerstorfer C, Logiewa A (2019) The upper size limit of the dust samples in road dust heavy metal studies: benefits of a combined sieving and air classification sample preparation procedure. *Environ Pollut* 245:1079–1085. <https://doi.org/10.1016/j.envpol.2018.10.131>
- Li F, Zhang J, Huang J, Huang D, Yang J, Song Y, Zeng G (2016a) Heavy metals in road dust from Xiandao District, Changsha City, China: characteristics, health risk assessment, and integrated source identification. *Environ Sci Pollut Res* 23:13100–13113. <https://doi.org/10.1007/s11356-016-6458-y>
- Li H, Shi A, Zhang X (2015) Particle size distribution and characteristics of heavy metals in road-deposited sediments from Beijing Olympic Park. *J Environ Sci* 32:228–237. <https://doi.org/10.1016/j.jes.2014.11.014>
- Li HH, Chen LJ, Yu L, Guo ZB, Shan CQ, Lin JQ, Gu YG, Yang ZB, Yang YX, Shao JR, Zhu XM, Cheng Z (2017) Pollution characteristics and risk assessment of human exposure to oral bioaccessibility of heavy metals via urban street dusts from different functional areas in Chengdu, China. *Sci Total Environ* 586:1076–1084. <https://doi.org/10.1016/j.scitotenv.2017.02.092>
- Li Y, Yu Y, Yang Z, Shen Z, Wang X, Cai Y (2016b) A comparison of metal distribution in surface dust and soil among super city, town, and rural area. *Environ Sci Pollut Res* 23:7849–7860. <https://doi.org/10.1007/s11356-015-5911-7>
- Lin H, Zhu X, Feng Q, Guo J, Sun X, Liang Y (2019) Pollution, sources, and bonding mechanism of mercury in street dust of a subtropical city, southern China. *Hum Ecol Risk Assess* 25:393–409. <https://doi.org/10.1080/10807039.2018.1526631>
- Liu A, Ma Y, Gunawardena JM, Egodawatta P, Ayoko GA, Goonetilleke A (2018) Heavy metals transport pathways: the importance of atmospheric pollution contributing to stormwater pollution. *Ecotoxicol Environ Saf* 164:696–703. <https://doi.org/10.1016/j.ecoenv.2018.08.072>
- Liu E, Wang X, Liu H, Liang M, Zhu Y, Li Z (2019) Chemical speciation, pollution and ecological risk of toxic metals in readily washed off road dust in a megacity (Nanjing), China. *Ecotoxicol Environ Saf* 173:381–392. <https://doi.org/10.1016/j.ecoenv.2019.02.019>
- Lu X, Wang L, Li LY, Lei K, Huang L, Kang D (2010) Multivariate statistical analysis of heavy metals in street dust of Baoji, NW China. *J Hazard Mater* 173:744–749. <https://doi.org/10.1016/j.jhazmat.2009.09.001>
- Ma WL, Zhu FJ, Liu LY, Jia HL, Yang M, Li YF (2019) PAHs in Chinese atmosphere: gas/particle partitioning. *Sci Total Environ* 693:133623. <https://doi.org/10.1016/j.scitotenv.2019.133623>
- Ma Y, Egodawatta P, McGree J, Liu A, Goonetilleke A (2016a) Human health risk assessment of heavy metals in urban stormwater. *Sci Total Environ* 557-558:764–772. <https://doi.org/10.1016/j.scitotenv.2016.03.067>
- Ma Z, Chen K, Li Z, Bi J, Huang L (2016b) Heavy metals in soils and road dusts in the mining areas of Western Suzhou, China: a preliminary identification of contaminated sites. *J Soils Sediments* 16:204–214. <https://doi.org/10.1007/s11368-015-1208-1>
- Men C, Liu R, Wang Q, Guo L, Miao Y, Shen Z (2019) Uncertainty analysis in source apportionment of heavy metals in road dust based on positive matrix factorization model and geographic information system. *Sci Total Environ* 652:27–39. <https://doi.org/10.1016/j.scitotenv.2018.10.212>
- Men C, Liu R, Wang Q, Guo L, Shen Z (2018a) The impact of seasonal varied human activity on characteristics and sources of heavy metals in metropolitan road dusts. *Sci Total Environ* 637-638:844–854. <https://doi.org/10.1016/j.scitotenv.2018.05.059>
- Men C, Liu R, Xu F, Wang Q, Guo L, Shen Z (2018b) Pollution characteristics, risk assessment, and source apportionment of heavy metals in road dust in Beijing, China. *Sci Total Environ* 612:138–147. <https://doi.org/10.1016/j.scitotenv.2017.08.123>
- Mohmand J, Eqani SAMAS, Fasola M, Alamdar A, Mustafa I, Ali N, Liu L, Peng S, Shen H (2015) Human exposure to toxic metals via contaminated dust: bio-accumulation trends and their potential risk estimation. *Chemosphere* 132:142–151. <https://doi.org/10.1016/j.chemosphere.2015.03.004>



- Müller G (1981) Die Schwermetallbelastung der Sedimente des Neckars und seiner Nebenflüsse Eine Bestandsaufnahme. *Chemiker-Zeitung* 6:157–164
- Naderizadeh Z, Khademi H, Ayoubi S (2016) Biomonitoring of atmospheric heavy metals pollution using dust deposited on date palm leaves in southwestern Iran. *Atmosfera*. <https://doi.org/10.20937/ATM.2016.29.02.04>
- Rahman MS, Khan MDH, Jolly YN, Kabir J, Akter S, Salam A (2019) Assessing risk to human health for heavy metal contamination through street dust in the Southeast Asian megacity: Dhaka, Bangladesh. *Sci Total Environ* 660:1610–1622. <https://doi.org/10.1016/j.scitotenv.2018.12.425>
- Roy S, Gupta SK, Prakash J, Habib G, Baudh K, Nasr M (2019) Ecological and human health risk assessment of heavy metal contamination in road dust in the National Capital Territory (NCT) of Delhi, India. *Environ Sci Pollut Res* 26:30413–30425. <https://doi.org/10.1007/s11356-019-06216-5>
- Shabanda IS, Koki IB, Low KH, Zain SM, Khor SM, Bakar NKA (2019) Daily exposure to toxic metals through urban road dust from industrial, commercial, heavy traffic, and residential areas in Petaling Jaya, Malaysia: a health risk assessment. *Environ Sci Pollut Res* 26:37193–37211. <https://doi.org/10.1007/s11356-019-06718-2>
- Shi G, Chen Z, Bi C, Wang L, Teng J, Li Y, Xu S (2011) A comparative study of health risk of potentially toxic metals in urban and suburban road dust in the most populated city of China. *Atmos Environ* 45:764–771. <https://doi.org/10.1016/j.atmosenv.2010.08.039>
- Shil S, Singh UK (2019) Health risk assessment and spatial variations of dissolved heavy metals and metalloids in a tropical river basin system. *Ecol Indic* 106:105455. <https://doi.org/10.1016/j.ecolind.2019.105455>
- Škrbić B, Đurišić-Mladenović N, Živančev J, Tadić Đ (2019) Seasonal occurrence and cancer risk assessment of polycyclic aromatic hydrocarbons in street dust from the Novi Sad City, Serbia. *Sci Total Environ* 647:191–203. <https://doi.org/10.1016/j.scitotenv.2018.07.442>
- Škrbić BD, Buljović M, Jovanović G, Antić I (2018) Seasonal, spatial variations and risk assessment of heavy elements in street dust from Novi Sad, Serbia. *Chemosphere* 205:452–462. <https://doi.org/10.1016/j.chemosphere.2018.04.124>
- Škrbić BD, Ji Y, Đurišić-Mladenović N, Zhao J (2016) Occurrence of the phthalate esters in soil and street dust samples from the Novi Sad City area, Serbia, and the influence on the children's and adults' exposure. *J Hazard Mater* 312:272–279. <https://doi.org/10.1016/j.jhazmat.2016.03.045>
- Soltani N, Keshavarzi B, Moore F, Tavakol T, Lahijanzadeh AR, Jaafarzadeh N, Kermani M (2015) Ecological and human health hazards of heavy metals and polycyclic aromatic hydrocarbons (PAHs) in road dust of Isfahan metropolis, Iran. *Sci Total Environ* 505:712–723. <https://doi.org/10.1016/j.scitotenv.2014.09.097>
- Srikanth K, Rao JV (2014) Spatial and seasonal variation of potential toxic elements in *Adocia pigmentifera*, seawater and sediment from Rameswaram, southeast coast of India. *Environ Earth Sci* 72:2905–2916. <https://doi.org/10.1007/s12665-014-3194-9>
- Taylor MP, Mackay AK, Hudson-Edwards KA, Holz E (2010) Soil Cd, Cu, Pb and Zn contaminants around Mount Isa city, Queensland, Australia: potential sources and risks to human health. *Appl Geochem* 25:841–855. <https://doi.org/10.1016/j.apgeochem.2010.03.003>
- Torghabeh AK, Jahandari A, Jamasb R (2019) Concentration, contamination level, source identification of selective trace elements in Shiraz atmospheric dust sediments (Fars Province, SW Iran). *Environ Sci Pollut Res* 26:6424–6435. <https://doi.org/10.1007/s11356-018-04100-2>
- Trujillo-González JM, Torres-Mora MA, Keesstra S, Brevik EC, Jiménez-Ballesta R (2016) Heavy metal accumulation related to population density in road dust samples taken from urban sites under different land uses. *Sci Total Environ* 553:636–642. <https://doi.org/10.1016/j.scitotenv.2016.02.101>
- USEPA (1989) Risk assessment guidance for superfund, vol. I: Human health evaluation manual. EPA/540/1-89/002. Office of Solid Waste and Emergency Response
- USEPA (1992) Guidelines for exposure assessment. Office of Research and Development, Office of Health and Environmental Assessment, Washington, DC; EPA/600/Z-92/001
- USEPA (1996) Soil screening guidance: technical background document. EPA/540/R-95/128. Office of Solid Waste and Emergency Response;
- USEPA (2001) Risk assessment guidance for superfund: volume III—part a, process for conducting probabilistic risk assessment. US Environmental Protection Agency, Washington, D.C. EPA/540/R-02/002
- USEPA (2003) Recommendations of the Technical Review Workgroup for lead for an approach to assessing risks associated with adult exposures to lead in soil. EPA/540/R-03/110
- USEPA (2007) Estimation of relative bioavailability of lead in soil and soil-like materials using in vivo and in vitro methods. Office of Solid Waste and Emergency Response, U.S. Environmental Protection Agency, Washington, DC
- USEPA (2009) Highlights of the child-specific exposure factors handbook. National Center for Environmental Assessment, Washington, DC. EPA/600/R-08/135
- USEPA (2017) Exposure factors handbook chapter 5 (update): soil and dust ingestion. U.S. EPA Office of Research and Development, Washington, DC. EPA/600/R-17/384
- Wahab MIA, Razak WMAA, Sahani M, Khan MF (2020) Characteristics and health effect of heavy metals on non-exhaust road dusts in Kuala Lumpur. *Sci Total Environ* 703:135535. <https://doi.org/10.1016/j.scitotenv.2019.135535>
- Wang G, Wang Y, Yin W, Xu T, Hu C, Chen J, Yuan J (2020) Seasonal exposure to PM<sub>2.5</sub>-bound polycyclic aromatic hydrocarbons and estimated lifetime risk of cancer: a pilot study. *Sci Total Environ*. <https://doi.org/10.1016/j.scitotenv.2019.135056>
- Wang J, Li S, Cui X, Li H, Qian X, Wang C, Sun Y (2016a) Bioaccessibility, sources and health risk assessment of trace metals in urban park dust in Nanjing, Southeast China. *Ecotoxicol Environ Saf* 128:161–170. <https://doi.org/10.1016/j.ecoenv.2016.02.020>
- Wang Q, Liu M, Li Y, Liu Y, Li S, Ge R (2016b) Dry and wet deposition of polycyclic aromatic hydrocarbons and comparison with typical media in urban system of Shanghai, China. *Atmos Environ* 144:175–181. <https://doi.org/10.1016/j.atmosenv.2016.08.079>
- Wang Q, Lu X, Pan H (2016c) Analysis of heavy metals in the resuspended road dusts from different functional areas in Xi'an, China. *Environ Sci Pollut Res* 23:19838–19846. <https://doi.org/10.1007/s11356-016-7200-5>
- Weerasundara L, Magana-Arachchi DN, Ziyath AM, Goonetilleke A, Vithanage M (2018) Health risk assessment of heavy metals in atmospheric deposition in a congested city environment in a developing country: Kandy City, Sri Lanka. *J Environ Manage* 220:198–206. <https://doi.org/10.1016/j.jenvman.2018.04.036>
- Wuana RA, Okieimen FE (2011) Heavy metals in contaminated soils: a review of sources, chemistry, risks and best available strategies for remediation. *ISRN Ecol* 2011:1–20
- Yang S, Li P, Liu J, Bi X, Ning Y, Wang S, Wang P (2019) Profiles, source identification and health risks of potentially toxic metals in pyrotechnic-related road dust during Chinese New Year.

- Ecotoxicol Environ Saf 184:109604. <https://doi.org/10.1016/j.ecoenv.2019.109604>
- Zafra C, Temprano J, Tejero I (2017) The physical factors affecting heavy metals accumulated in the sediment deposited on road surfaces in dry weather: a review. *Urban Water J* 14:639–649. <https://doi.org/10.1080/1573062X.2016.1223320>
- Zhang N, Han B, He F, Xu J, Niu C, Zhou J et al (2015) Characterization, health risk of heavy metals, and source apportionment of atmospheric PM 2.5 to children in summer and winter: an exposure panel study in Tianjin, China. *Air Qual Atmos Health*. <https://doi.org/10.1007/s11869-014-0289-0>
- Zhao H, Li X, Wang X, Tian D (2010) Grain size distribution of road-deposited sediment and its contribution to heavy metal pollution in urban runoff in Beijing, China. *J Hazard Mater* 183:203–210. <https://doi.org/10.1016/j.jhazmat.2010.07.012>
- Zhao H, Zhao J, Yin C, Li X (2014) Index models to evaluate the potential metal pollution contribution from wash off of road-deposited sediment. *Water Res* 59:71–79. <https://doi.org/10.1016/j.watres.2014.04.012>

**Publisher's note** Springer Nature remains neutral with regard to jurisdictional claims in published maps and institutional affiliations.